Journal of Experimental Marine Biology and Ecology 452 (2014) 31–39

Contents lists available at ScienceDirect

Journal of Experimental Marine Biology and Ecology

journal homepage: www.elsevier.com/locate/jembe

Cell death and aggregate formation in the giant diatom *Coscinodiscus wailesii* (Gran & Angst, 1931)

Linda H. Armbrecht [a,*], Victor Smetacek [a], Philipp Assmy [a,b], Christine Klaas [a]

[a] Alfred Wegener Institute Helmholtz Centre for Polar and Marine Research, Am Handelshafen 12, 27570 Bremerhaven, Germany
[b] Norwegian Polar Institute, Fram Centre, Hjalmar Johansens gt. 14, 9296 Tromsø, Norway

ARTICLE INFO

Article history:
Received 19 August 2013
Received in revised form 3 December 2013
Accepted 4 December 2013
Available online xxxx

Keywords:
Autolysed cytoplasm
Diatom cell death
Polysaccharide layer
Silicic acid limitation
SYTOX® Green
Transparent exopolymer particles

ABSTRACT

The demise phase of diatom blooms following nutrient exhaustion is characterised by the formation of aggregates with high sinking rates that facilitate carbon export to the seafloor. However, the nature of the binding substances involved and the physiological status of the phytoplankton during aggregation are not well established. Transparent Exopolymer Particles (TEP), exudated by living cells, have been proposed as a binding agent of aggregates but autolysed cytoplasm released after cell death might also play such a role. To differentiate these processes we studied the response of cultures of the mucilage and TEP-producing giant diatom *Coscinodiscus wailesii* to nutrient, in particular silicic acid, limitation. Two staining methods were applied: SYTOX® Green to follow cell viability and cell death and Alcian Blue (AB) to quantify the production of TEP. Large aggregates formed exclusively in cultures with high cell densities in which the SYTOX® Green signal increased during the senescence phase. TEP-production under nutrient replete (f/2 treatment) and nitrate reduced growth conditions (f/2-N treatment) with high cell densities was comparatively low, indicating reduced photosynthetic activity in the stationary and senescent phases. In contrast, TEP-production was enhanced in low-density Si-limited cultures (f/2-Si treatment), probably as a means to discharge excess photosynthate, as the cells were densely packed with chloroplasts. The C/N ratios of aggregated and solitary cells did not differ significantly indicating that the binding agent was not mainly polysaccharidic. We propose that aggregate formation in *C. wailesii* is a consequence of cell lysis after cell death and that autolysed cytoplasm is the binding agent rather than TEP. This would imply that cell lysis plays a substantial role in bloom termination and mucilage formation in *C. wailesii*, which would in turn influence biogeochemical cycling in regions where this diatom thrives.

1. Introduction

In shelf and coastal ecosystems phytoplankton blooms grow until nutrient exhaustion and subsequently form rapidly sinking aggregates that settle out of the surface layer (Smetacek, 1985; Thornton, 2002). Despite the ecological and biogeochemical importance of this process little is known about the mechanisms triggering aggregate formation. In particular it is unresolved whether cell death occurs prior to aggregate formation and what the nature of the aggregate-binding agents is. Although nitrogen and phosphorus depletion have been suggested to cause bloom termination in marine coastal waters, there is still no consensus regarding the true limiting nutrient as the bloom demise further depends on local conditions (e.g. eutrophication) and species composition (Hecky and Kilham, 1988).

It was widely believed that cells either die by necrosis due to nutrient exhaustion or are killed by grazing or viral attack (Bratbak et al., 1993; Fuhrmann, 1999). The discovery that programmed cell death (PCD) in phytoplankton can be induced by environmental and physiological stress such as nutrient limitation, age, increased salinity or oxidative stress has cast a new light on phytoplankton life history and population ecology (Bidle and Falkowski, 2004). Metacaspases (orthologues of caspases, the death-mediating proteins of the apoptotic machinery in multicellular organisms (Uren et al., 2000), were detected in auto- and heterotrophic unicellular phytoplankton (e.g. Bidle and Bender, 2008; Vardi et al., 1999). PCD in phytoplankton is a form of autocatalytic cell suicide involving morphological changes and biogeochemical pathways known from apoptosis, ultimately leading to the lysis of the cell (Bidle and Falkowski, 2004). Cell lysis has been previously reported to play an important role in phytoplankton bloom termination, occasionally resulting in large-scale mucilage formation (Baldi et al., 1997; Lancelot, 1995). It has been earlier speculated that cellular material enhances the coagulation of aggregates (Hargraves and French, 1983).

On the other hand, exudation of transparent exopolymer particles (TEP), a special class of exopolymeric substances (EPS), has been suggested to promote aggregate formation due to their sticky nature

Abbreviations: AB, Alcian Blue; EPS, Exopolymeric Substances; PCD, Programmed Cell Death; TEP, Transparent Exopolymer Particles; LC, Live Cells; DC, Dead Cells; DCCM, Dead Cells containing Cellular Material; EF, Empty Frustules.

* Corresponding author at: Macquarie University, Faculty of Science, Department of Biological Sciences, Eastern Road, North Ryde NSW 2109, Australia. Tel.: +61 9850 8205.

0022-0981/$ – see front matter © 2013 Elsevier B.V. All rights reserved.
http://dx.doi.org/10.1016/j.jembe.2013.12.004

(Alldredge et al., 1993). These particles consist of acidic, surface active polysaccharides that clump together with ambient particles such as bacteria, phytoplankton, detritus or mineral clays (Engel, 2009; Passow, 2002; Passow et al., 2001). Size classes of TEP range from micro- up to millimeter scales and by forming dense networks they can even span several centimeters (Azetsu-Scott and Passow, 2004; Engel, 2009). As they are actively released by growing bacteria or phytoplankton, considering TEP as the aggregate-stabilizing agent would imply that mainly living cells sink out (Decho, 1990; Passow and Alldredge, 1994). The physiological state of the sinking cells has different consequences for the elemental cycling and downward transport to the seafloor: While the mass sinking of living cells enhances the downward flux of carbon and nitrogen, the sinking of empty diatom frustules results in export of silica to the deep ocean (Assmy et al., 2013).

Coscinodiscus wailesii (Coscinodiscaceae), a large centric diatom (175–500 μm in diameter), has been shown to produce mucilage as well as TEP (Engel and Passow, 2001). The species was reported in European waters for the first time in 1977 when it caused an extensive mucilage-phenomenon following a bloom in the English Channel (Boalch and Harbour, 1977) and has established itself permanently in the North Sea since then (Edwards et al., 2001). The mucilage was described as a greyish, highly sticky material, heavily loaded with plankton remains and other solid particles, which clogged and ripped fishing nets and restricted trawling activities (Boalch and Harbour, 1977). A high content of highly branched heteropolysaccharides were found in the extracellular releases of the diatom in culture (Percival et al., 1980). Therefore, it might be assumed that TEP formed the matrix of the mucilage as has been proposed for *C. granii*, a related species of *C. wailesii* (Fukao et al., 2009). Nevertheless, investigations of *C. wailesii* in its new natural habitat remain difficult, as it occurs sporadically in some years and is absent in others. Elevated temperature and "anomalous physical and biological conditions" have been suggested to facilitate its invasion along European coasts (Edwards et al., 2001; Gohin et al., 2003).

In this study *C. wailesii* was grown at different nutrient concentrations in order to follow the patterns of growth and senescence as a function of silicic acid availability (Alcoverro et al., 2000; Myklestad, 1974, 1995). The main aims of the experiments were: 1. To investigate the role of cell death during aggregation (Veldhuis et al., 2001). 2. To identify a potential link between aggregate formation and the binding substances involved, i. e. TEP and/or autolysed cytoplasm. 3. To examine feedbacks between nutrient utilisation, growth and aggregation in *C. wailesii*.

2. Methods

2.1. Cultures

Single *C. wailesii* cells were isolated from a plankton sample collected on board RV Aade using a hand-net (80 μm mesh size) at the permanent sampling station Helgoland Roads in the North Sea (54°11′N, 7°54′E) in February 2010. Non-axenic cultures were grown in tissue culture test plates (Orange Scientific) at 19 °C and an irradiance of 20 μmol photons m^{-2} s^{-1}. The best growing clone was selected for the experiment, allowing direct comparisons between treatments without having to account for strain- or physiological state-dependent variation. When the growth experiment was started all *C. wailesii* cells measured approximately 330 μm in diameter.

2.2. Media

Experimental media (Table 1) were prepared from fresh North Sea water obtained in April 2010 containing initial nutrient concentrations of 20 μM nitrate, 3 μM phosphate and 5 μM silicic acid. f/2 medium was prepared according to Guillard and Ryther (1962) with a final concentration of 50 μmol L^{-1} of silicic acid. Low silicic acid media (f/2-Si) was prepared likewise without addition of sodium silicate. An additional treatment (f/2-N) with a nitrate concentration similar to natural conditions and a Si:N of ~2 (see Table 1 for Si:N ratios of the other two media) was prepared by enriching North Sea water with modified f/2 (without nitrate addition and a final concentration of 50 μmol L^{-1} silicic acid). Media were sterile filtered (0.1 μm) into 1 L autoclaved narrow-mouthed polycarbonate bottles (Nalgene Nunc. International, USA).

Table 1
Nutrient conditions of at the start and end of the growth experiment. Nutrient concentrations (μM) in f/2, f/2-N and f/2-Si media at the start (n = 1) and at the end (n = 3) of the growth experiment. (N) nitrate + nitrite + ammonium concentrations, whereby ammonium values were close to detection limit. (P) Phosphate concentrations. (Si) Silicic acid concentrations, values in brackets correspond to the initial Si:N molar ratio.

	Media	N	P	Si
Start	f/2	684	28.3	48.1 (0.07)
	f/2-N	22	31.1	46.5 (2.1)
	f/2-Si	759	32	5.29 (0.007)
End	f/2	669 ± 21	21 ± 2	2.0 ± 0.5
	f/2-N	5 ± 2	24.8 ± 0.8	1.5 ± 0.4
	f/2-Si	731 ± 31	30 ± 1	1.4 ± 0.3

2.3. Set-up of growth experiment

Prior to the experiment, cells were acclimated to the experimental conditions for 20 days in sterile 70 mL polystyrene tissue culture flasks (Corning Inc., USA) to gain sufficient cells for the experiment. The growth experiment was conducted at 15 °C and an irradiance of 50 μmol photons m^{-2} s^{-1} (OSRAM L 58W/965, Biolux, Germany) and a light:dark cycle of 16:8 h. All cultures were slowly (1.6 rpm) rotated on a plankton wheel to maintain them in suspension and to enhance the probability of particle collision, a prerequisite for aggregate formation besides particle size, form, density and stickiness (Hamm, 2002). As light was provided from only one side of the plankton wheel light intensity ranged from a maximum of 80 μmol m^{-2} s^{-1} at the bottom to a minimum irradiance of 20 μmol m^{-2} s^{-1} at the top of the plankton wheel. Six replicate cultures were grown for each nutrient condition (f/2, f/2-N and f/2-Si) in 1 L polycarbonate bottles (Nalgene Nunc. International, USA) at an initial concentration of 25 cells mL^{-1}. Three of the replicate cultures (a, b, c, batch 1) were sampled during exponential and stationary phase (8 and 16 days after starting incubations, respectively) while the three remaining replicates (a, b, c, batch 2) were sampled during the senescent phase (at the end of each incubation). Sampling was undertaken for analysis of TEP, particulate organic carbon (POC) and nitrogen (PON), nitrate + nitrite + ammonium (hereafter total N), phosphate and silicate. Dissolved nutrients of the culture media at the start and at the end of the experiment were analysed following Grasshoff et al. (1999). For all other sampling procedures see Sections 2.4–2.10.

2.4. Abundance

In order to follow growth phases of *C. wailesii* cultures, cell numbers were determined by microscopy (Axiovert 200, Zeiss, Oberkochen, Germany) in unfixed samples at two-day intervals. Prior to counting, 50 mL subsamples were settled into Utermöhl chambers (HydroBios, Kiel, Germany) for 4 h. When cell density increased in f/2 and f/2-N media (at day 12 of the experiment) the sampling volume for cultures grown under these nutrient conditions was reduced to 25 mL and the settling time to 2 h. Settling times of 4 and 2 h were observed to be sufficient for all cells to settle. However, during the exponential growth phase *C. wailesii* cells were occasionally found to be neutrally buoyant and a small number of cells (<7 cells) remained in the settling column, even after 4 h of sedimentation. In eight subsamples of the f/2 and f/2-N cultures small aggregates containing ~20 cells were observed to not sediment. As these small aggregates and the single neutrally buoyant

cells occurred in high cell density cultures and accounted for a very small fraction of the total cell number, they were neglected.

Cells were counted at 100× magnification, resulting in few cells (~23–60) being counted in the first 4 days of the experiment until cells started to grow exponentially. After day 10 approximately 200 cells were counted in each sedimented subsample, with the exception of *C. wailesii* cells grown in f/2-Si medium that had lower cell densities (<100 cells per 50 mL; see results Section 3.1).

2.5. Cell viability (staining with SYTOX® Green)

In order to follow the physiological status of *C. wailesii* cultures, unfixed cells were stained with SYTOX® Green (Invitrogen™) at a final concentration of 0.5 μM for 15 min prior to counting under epifluorescent light after settling in Utermöhl chambers as above. The samples were incubated in the dark with the fluorescent dye under a fume hood. Cells were categorised according to their fluorescence signal into live cells (LC), which showed a bright red autofluorescent signal (chlorophyll) under epifluorescence microscopy, dead cells containing cellular material (DCCM) which had a partly red, partly green fluorescence signal, dead cells (DC) with a bright green signal generated by the SYTOX® Green stain. The fraction of cellular material within dead cells ranged from one fifth of the frustule volume to completely filled frustules. Empty frustules (EF) were counted separately in the same samples using light microscopy.

2.6. Aggregate formation

The presence and size of aggregates was determined visually every second day prior to counting. During exponential and stationary growth phases the three batch 1 replicate cultures of each treatment and thereafter the three batch 2 replicates were examined. Until day 12 when noticeable aggregates started to form (see Results) aggregate formation was documented by photographing subsamples of *C. wailesii* cultures used for counting.

2.7. Transparent Exopolymer Particles (TEP)

Sampling for TEP took place on day 8 during the exponential phase, on day 16 during the stationary phase and on the last day of the experiment for each nutrient condition during the senescent phase.

2.7.1. Microscope analysis

Duplicate Alcian Blue (AB) stained and blank filters were prepared from 5 to 20 mL of cultures (depending on pre-evaluation of particle density by microscopy) during exponential, stationary and senescent phases and fixed onto Cyto Clear Slides (Osmonics Inc.) for analysis by microscopy as described in Alldredge et al. (1993) and using the Filter-Transfer-Freeze technique (Hewes and Holm-Hansen, 1983). See Engel (2009) for a detailed description of both techniques. Due to large variation in size of TEP produced by *C. wailesii,* the abundance of small TEP (<150 μm) was calculated as described in Engel (2009) using an Axioskop 2 plus compound microscope and a colour digital camera (AxioCam HRa, Zeiss). Large TEP (>150 μm) were counted at 100× magnification under the same microscope.

2.7.2. Colorimetric analysis

TEP produced by *C. wailesii* showed extremely high variations in size during stationary and senescent phases. Therefore, for these phases, additional filter samples (10–30 mL) were taken for colorimetric analysis of TEP after the method described in Passow and Alldredge (1995) and Engel (2009). The semi-quantitative method detects TEP photometrically, independent of their size. The amount of Alcian Blue adsorbed to particles is directly related to the equivalent weight of the polysaccharide Gum Xanthan, which is used as a standard.

2.8. Carbon content of TEP (TEP-C_{color})

The carbon content of gel particles (TEP-C) was estimated from colorimetrically determined TEP concentrations (as these seemed more accurate, see Results) using the following conversion factor for *C. wailesii* (Engel and Passow, 2001):

$$\text{Carbon}\ \left[\mu g\ L^{-1}\right] = \left(0.88 \pm 0.24\right)\ \left[\text{TEP};\ \mu g\ \text{Xeq.}\ L^{-1}\right] \quad (1)$$

Subsequently, the contribution of TEP-C_{color} to total particulate organic carbon (POC) was determined for the stationary and senescent phases.

2.9. Particulate organic carbon (POC) and nitrogen (PON)

Depending on cell density, a 35–300 mL subsample from each incubation bottle was filtered under low vacuum pressure (~150 mmHg) onto 25 mm pre-combusted (500 °C, 12 h) GF/F filters (Whatman). Filters were stored in 1.5 mL Eppendorf-tubes (Eppendorf), dried at 60 °C for 42 h and subsequently stored in an exsiccator until further analysis. A subsample was fixed with Lugol's solution and counted with the Utermöhl method in order to estimate cellular carbon and nitrogen content. For POC/PON analysis, filters were wrapped in tin foil and analyzed in a CHN-Analyzer (Euro Elemental Analyzer, Eurovector Instruments & Software). Due to very low cell densities in silicic acid-limited incubations, samples from the three replicate incubations during the senescent phase were pooled in order to gain enough material for POC/PON analysis.

2.10. Comparison of POC/PON of aggregates versus suspended cells

To compare POC and PON contents of aggregates *versus* suspended cells, seven additional 12–14 day old *C. wailesii* cultures (all maintained in f/2 medium) were transferred to a plankton wheel for two days. Temperature and light conditions were similar to previous incubations. After 2 days all aggregates that had formed within each bottle were picked separately and filtered with a small amount (5–10 mL) of the respective culture medium onto pre-combusted GF/F filters (as in 2.9). Depending on the density of the suspended cells 70–130 mL were filtered. The fraction containing the aggregates constituted 4–7% of the total filtered sampling volume. Average cell density in the incubation bottles (including aggregates) was determined after mixing the culture medium and counting using the Utermöhl method as described in Section 2.4 after fixation with Lugol's solution.

2.11. Statistics

Two-tailed t-tests were conducted to test for significant differences of growth rates of *C. wailesii* grown under different nutrient conditions. Full-Factor Analyses of Variance were carried out to test the combined effect of "Phase of culture" (exponential, stationary, senescent) and "Nutrient condition" (f/2, f/2-N, f/2-Si) on growth. In the case of significant effects additional Tukey Honest Significance (HSD) tests were performed in order to determine the effect of each individual factor. Statistical analyses were conducted using the SAS software JMP® 8.

As the number of replicates was usually $n = 3$, homogeneity of variances was assumed for all statistical tests.

3. Results

3.1. Growth response

After a lag phase of 2 to 4 days *C. wailesii* grew exponentially in all treatments albeit at different rates (Fig. 1). In f/2 and f/2-N average growth rates during exponential phase were similar ($0.40 \pm 0.08\ d^{-1}$ and $0.42 \pm 0.04\ d^{-1}$, respectively, $p = 0.7$) while cells in the f/2-Si treatments showed significantly lower growth rates ($0.21 \pm 0.02\ d^{-1}$,

$p_{f/2,f/2\text{-}Si} < 0.05$ and $p_{f/2\text{-}N,f/2\text{-}Si} < 0.01$). Despite low ambient Si concentrations in the f/2-Si treatments, cells grew continuously until days 12–14 and reached the stationary phase 2 to 4 days later than cultures grown in f/2 and f/2-N (Fig. 1). Measurements of nutrient concentrations at the end of the experiment (Table 1) indicate that, in all treatments, growth was limited by silicic-acid availability although nitrate might also have been limiting in the f/2-N treatment. Si:N uptake ratios of 3.1, 2.6 and 0.1 could be estimated from the difference between initial ($n = 1$) and final ($n = 3$) silicate and total N, (i.e. $NO_2 + NO_3 + NH_4$) concentrations in the f/2, f/2-N and f/2-Si treatment, respectively (Table 1). Si:N uptake ratios based on maximum PON stocks measured (senescent phase) and Si decrease in the media (Table 1) gave uptake ratios of 1.2, 2.9 and 0.3 for the f/2, f/2-N and f/2-Si treatment, respectively. With the exception of the f/2 treatment, the Si:N uptake calculated using both methods are quite similar indicating that little PON remineralisation occurred during the experiments. As a consequence, Si:N uptake ratios estimated using changes in dissolved Si and PON concentrations should be more reliable than estimates from nutrient N deficit for the f/2 treatment due to the very high N concentrations remaining in the media.

The SYTOX® Green staining approach and the classification in DC, DCCM and EF during growth of *C. wailesii* allowed us to closely follow the physiological status of individual cells in the different treatments. The number of dead and empty cells was high during the lag phase, possibly reflecting cell damage during manipulation of cultures as the proportion of dead and empty cells decreased rapidly during the exponential growth phase in all treatments (Fig. 2). Dead and empty cells became more prominent again after day 20 in all treatments indicating that incubations had entered the senescent phase. While in cultures grown under f/2 and f/2-Si conditions the proportion of non-viable cells increased exponentially after day 20 reaching over 50% of total cell population at the end of the experiment, the proportion of non-viable cells in f/2-N media increased linearly and most cells were still viable on day 30 (Fig. 2). *C. wailesii* cells grown under f/2-Si nutrient conditions were characterised by a noticeable colour change, becoming almost opaque, due to accumulation of cytoplasm and (at least partly) of pigments in chloroplasts (Fig. 3).

3.2. Aggregate formation

Before day 6 of the experiment, no aggregates were observed in the *C. wailesii* cultures. Smaller aggregates, containing approximately 20–50 cells, were sporadically observed between days 6 and 12 (during the exponential growth phase) in the f/2 and f/2-N triplicates but not in the f/2-Si treatments. Formation of larger aggregates (0.5 cm in diameter to thin thread-like aggregates of up to 10 cm in length) occurred from day 12 until the end of the experiment in all treatments except f/2-Si. In the latter treatment we found only few very small aggregates containing approximately 5–10 cells after day 12.

The formation process of aggregates was also followed closely under the microscope. Mucilaginous aggregates were formed through the release of cellular material into the ambient seawater followed by scavenging of live cells and empty frustules. The process of cytoplasm release is shown in Fig. 4A–D. Live and dead cells were embedded in a dense matrix constituted by the released brownish cytoplasm material forming the large aggregates found in f/2 and f/2-N media after day 12. Cell densities were low in the f/2-Si treatment which is probably why aggregates were not formed. Further microscopic analysis of AB stained particles revealed thread-like structures, also brownish in colour and with TEP particles adhering exclusively on their surface but without any incorporation into the mucous matrix (Fig. 5). These stained threads were found sporadically in the f/2 treatment and to a lesser extent in the f/2-N treatment. In the f/2-Si treatment none of

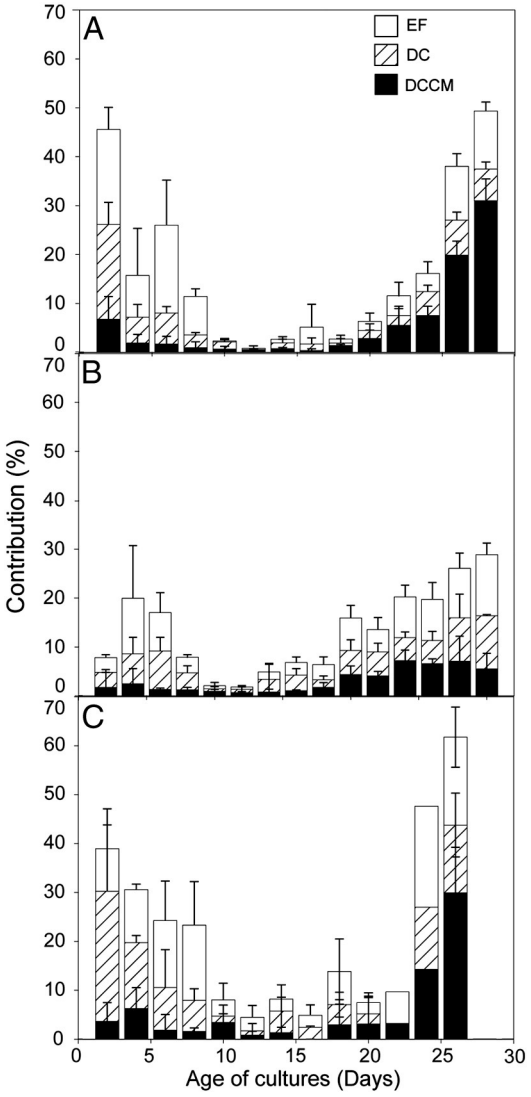

Fig. 2. Portions of non-living *Coscinodiscus wailesii* cells under different nutrient conditions. Contribution (in %) of dead cells containing cellular material (DCCM), dead cells (DC) and empty frustules (EF) to total cell concentrations. A) f/2, B) f/2-N, C) f/2-Si. Error bars represent one standard deviation based on 3 samples from triplicate incubations (except for f/2-Si on days 22 and 24 were a sample from one batch only was counted).

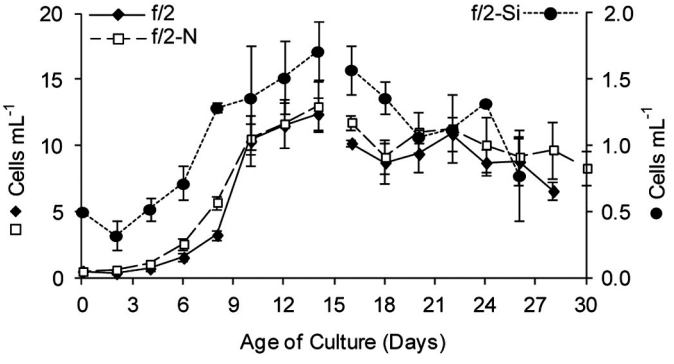

Fig. 1. Growth of *Coscinodiscus wailesii*. Temporal evolution of live cell concentrations for the f/2, f/2-N and f/2-Si treatments. Note difference in cell abundances for f/2 and f/2-N (left scale) and f/2-Si (right scale) treatments. Samples from exponential and stationary phase were taken from one batch consisting of 3 replicate incubations for each treatment (before day 16), while samples at the end of incubations (senescent phase) were taken from a second batch of 3 replicates each. Due to the low cell density in f/2-Si treatments, replicates from the second batch on days 22 and 24 were pooled.

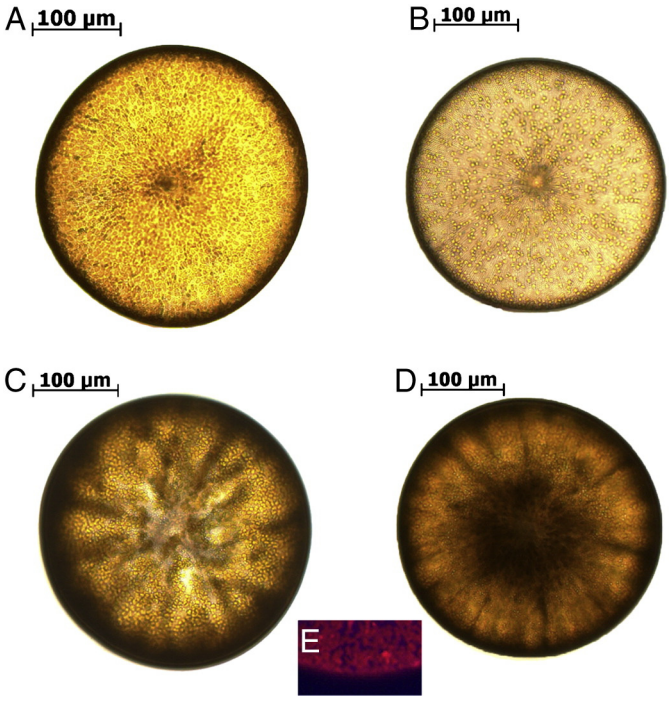

Fig. 3. Cells of *Coscinodiscus wailesii* under different nutrient conditions. *C. wailesii* cells grown in A) f/2, day 16, B) f/2-N, day 20, C) f/2-Si, day 16, D) f/2-Si, day 20. Insert (E) shows chloroplasts under epifluorescence in f/2-Si treatments (insert from panel D).

these stained filamentous structures were observed. We cannot rule out that the released cellular material in the low-density f/2-Si treatment (Fig. 4A–B) could have been the binding agent of the small 5–10 cell aggregates observed after day 12 but presume that most of the released material was rapidly diluted in the ambient medium, which might be a further reason for absence of large aggregates.

3.3. Transparent Exopolymer Particles (TEP)

The total abundance of TEP L^{-1} determined by microscope analysis of AB stained particles as well as colorimetric TEP (TEP_{color}, µg Xeq. L^{-1}) increased continuously from the exponential over the stationary to the senescent phase in all cultures (Fig. 6A,B). TEP abundances and colorimetric TEP showed, however, different patterns (in particular during senescence) for the different treatments: TEP abundances were highest in f/2-Si followed by f/2-N and f/2 (Fig. 6A), while TEP_{color} concentrations were higher in the f/2 treatment followed by f/2-N and f/2-Si (Fig. 6B). These results indicate differences in TEP sizes between incubations in f/2-Si and the other treatments, also observed in counts of small vs. large (>150 µm) TEP.

On a cellular basis, silicic acid-limited treatments showed a significantly higher abundance of TEP during the senescent phase than any other treatment and growth phase (Fig. 6C; Tukey HSD, each $p < 0.001$). No significant differences in the abundance of TEP were determined between cells grown in f/2 and f/2-N during similar growth phases (Tukey HSD, each $p > 0.9931$, Fig. 6C). Cell-normalised TEP_{color} concentrations followed similar pattern (Fig. 6D), although differences were not as marked. TEP_{color} concentrations per cells were significantly higher in the senescent silicic acid-limited treatment than values for all other treatments (both stationary and senescent phases) except for the senescent f/2 treatment (Fig. 6D; Tukey HSD, $p_{Sen,f/2\text{-}Si;Stat,f/2} = 0.0013$, $p_{Sen,f/2\text{-}Si;Stat,f/2\text{-}N} = 0.0003$, $p_{Sen,f/2\text{-}Si;Stat,f/2\text{-}Si} = 0.0008$, $p_{Sen,f/2\text{-}Si;Sen,f/2\text{-}N}$).

In addition to cytoplasmic strands described above (Section 3.2, Fig. 5), live cells were also covered by a polysaccharide layer that was stained by AB (Fig. 7A,B). The membrane-like polysaccharide layer was frequently observed separated from the frustule (Fig. 7C–F), resembling moulds of the different components of the frustule: the whole frustule (Fig. 7C), girdle bands associated to the valve (Fig. 7D–E) or individual

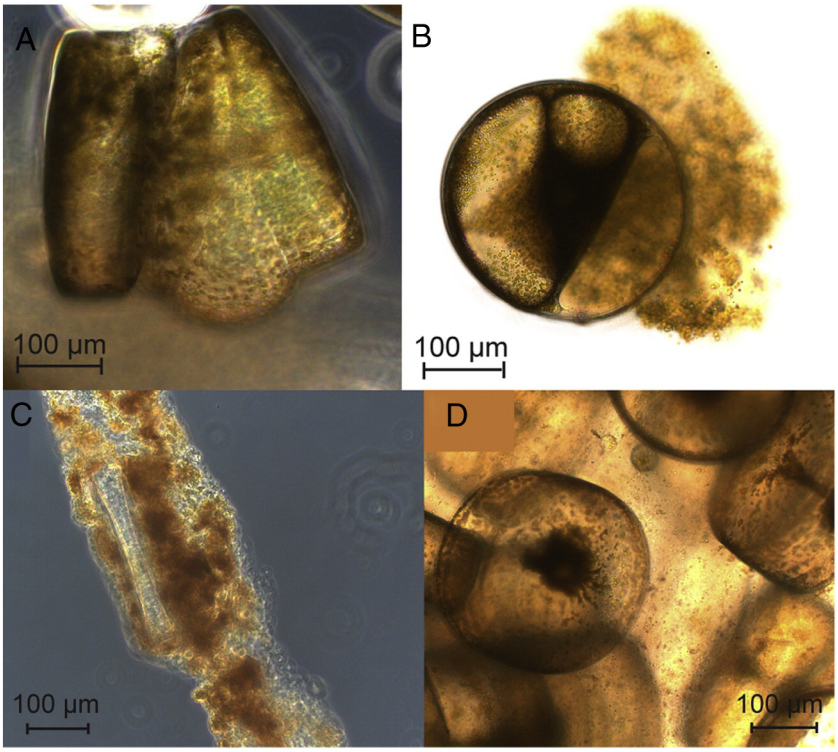

Fig. 4. Aggregate formation in *Coscinodiscus wailesii*. Aggregate formation after cell lysis and cytoplasm release during stationary growth and senescence of *C. wailesii*. A) *C. wailesii* cell opening laterally and releasing cytoplasm to the ambient medium (f/2-Si, day 26). B) *C. wailesii* cell with partly released cytoplasm (f/2-Si, day 26). C) Empty frustule captured in filamentous mucilaginous material (f/2, day 16). D) Dense aggregate matrix observed in f/2 and f/2-N treatments containing live and dead *C. wailesii* cells (f/2, day 26).

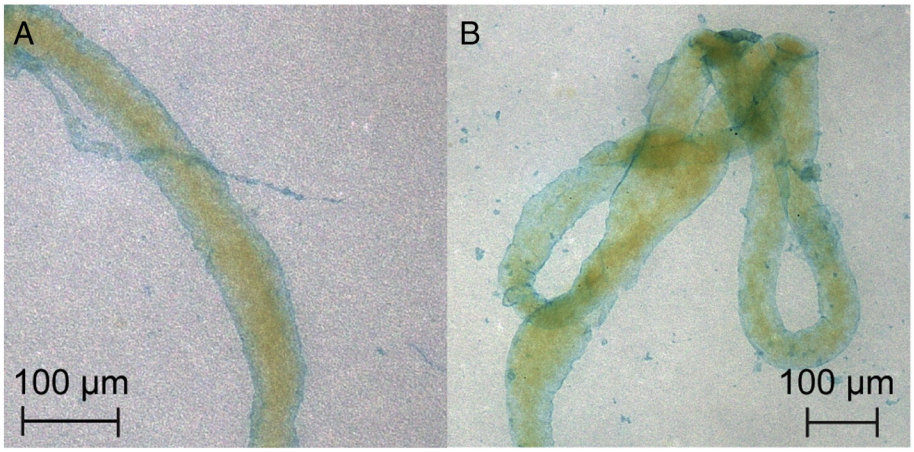

Fig. 5. TEP-covered cytoplasmic threads produced by *Coscinodiscus wailesii*. TEP on the surface is indicated by the Alcian-blue stain. Picture taken from A) f/2 b, batch 1. B) f/2 c, batch 1.

valves (Fig. 7F). In the exponential phase of the f/2 treatment, we found only moulds (no stained full or empty cell) while during the stationary and senescent phase we found both, moulds and live cells with the AB-stained layer. In f/2-N treatments we found structures that might have been parts of the moulds during the stationary phase and both, moulds and live cells with the AB-stained layer during senescence. In the f/2-Si treatment, we observed moulds only during the senescence phase. Because cell concentrations were already at their highest in the stationary phase in f/2 and f/2-N while TEP_{color} was highest during senescence, it is unlikely that moulds contributed significantly to TEP concentrations.

3.4. Composition of particulate matter

POC and PON concentrations increased from exponential to stationary growth phase, following the increase in *C. wailesii* cell abundance (Fig. 8). Nutrient limitation in the stationary phase of all treatments led to a shift towards higher C:N ratios as typically observed in nutrient limited phytoplankton (Geider and Roche, 2002). Highest C:N ratios during exponential growth were found in f/2-Si (7.8 ± 0.4 s.d.) followed by f/2 (5.8 ± 0.8 s.d.) and f/2-N (4.9 ± 0.2 s.d.) and during stationary growth in f/2-N (17 ± 2 s.d.) followed by f/2-Si (15.0 ± 0.2 s.d.) and f/2 (10 ± 0.4 s.d.). During senescence, C:N ratios in f/2 and f/2–Si decreased as compared to the stationary phase (8.4 ± 0.6 s.d. and 8.6, respectively) but remained high in the f/2-N treatment (16 ± 1 s.d.), possibly reflecting freshly extruded cytoplasm due to increased cell mortality in the senescent phase in f/2 and f/2-Si. Despite the observed shifts in C:N ratios, no large differences were observed in POC and PON concentrations between stationary and senescent phases in both f/2 and f/2-N (Fig. 8) and only minor changes were observed in the f/2-Si treatments despite the large increase in the proportion of dead cells in all treatments. These results further suggest that the bulk of particulate matter originated from released cytoplasm after cell death.

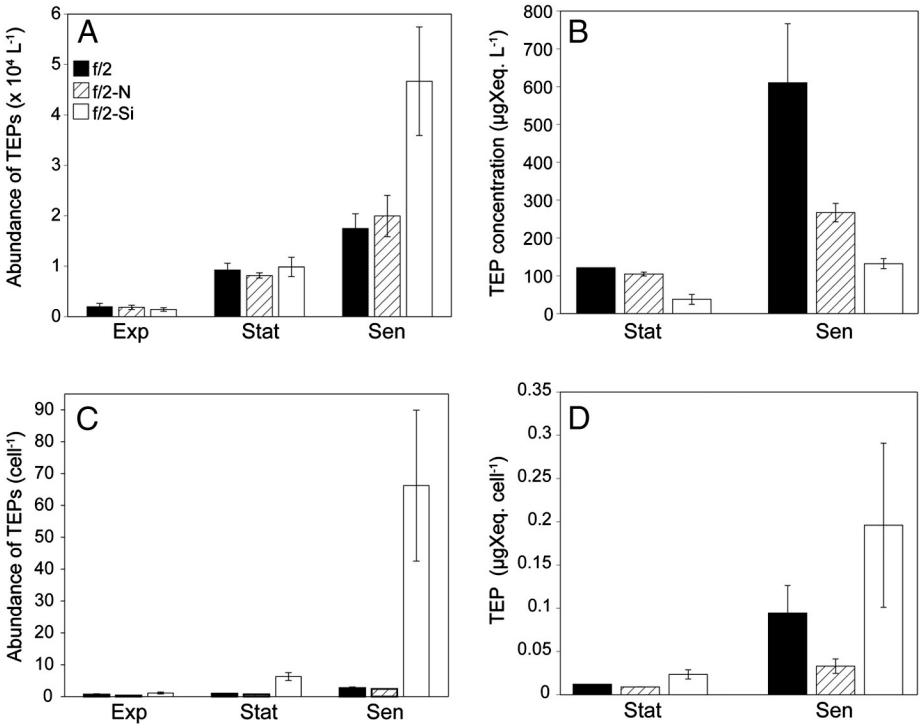

Fig. 6. TEP produced during growth of *Coscinodiscus wailesii* under different nutrient conditions (TEP abundance and concentration). A) Microscopically determined mean abundance of TEP (number of particles L^{-1}) during exponential (Exp), stationary (Stat) and senescent (Sen) phases, B) photometrically determined mean concentration of TEP_{color} (µg Xeq. L^{-1}) during Stat and Sen produced by *C. wailesii* under nutrient-replete (f/2), low Si:N (f/2-N) and silicic acid-limited (f/2-Si) conditions. Each n = 3, except in b) $n_{Stat,f/2} = 2$. Each error bar represents 1 standard deviation from the mean. C) and D) TEP abundances and concentrations as in A) and B) but normalised per cell.

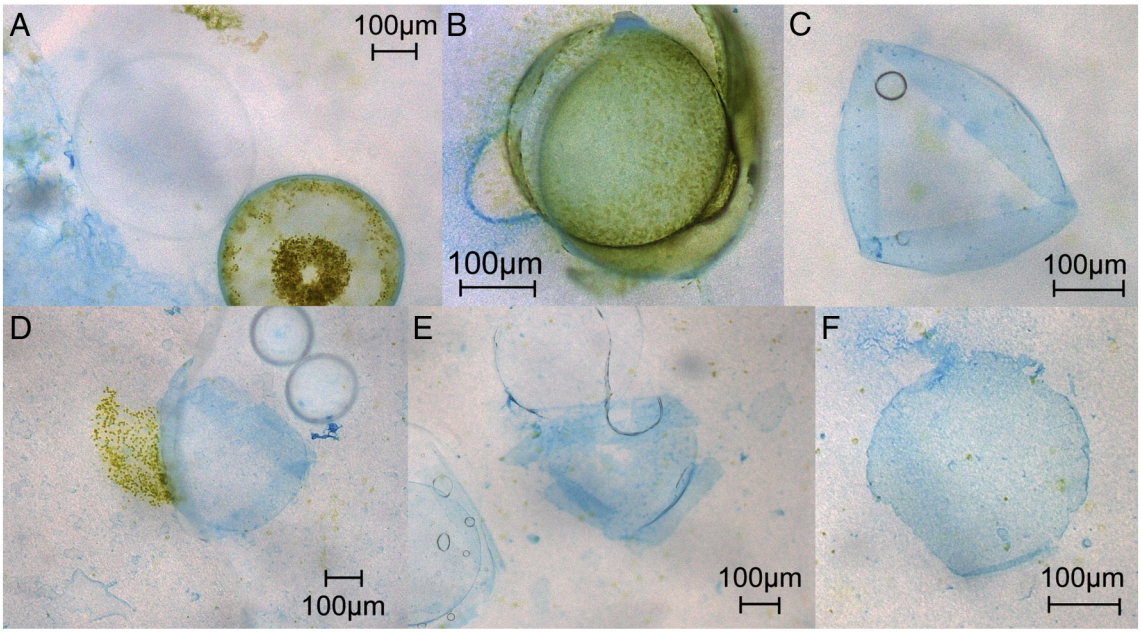

Fig. 7. Polysaccharide layer covering *Coscinodiscus wailesii* frustules visualised by Alcian-Blue staining. Intact polysaccharide layer enclosing living cells of *C. wailesii* (A), cellular material (B) and sloughed off layers resembling moulds of the valve and girdle bands (B–F). Photos taken from A) f/2-N a, batch 2, B) f2 a, batch 1, C–F) f/2-Si c, batch 2.

This is further supported by molar C:N ratios determined in additional f/2 incubations at the beginning of the stationary phase with values of 7.81 ± 2.41 s.d. for aggregates and 6.53 ± 1.81 s.d. for suspended, solitary cells. Although C:N ratios of aggregates were higher, there was no significant difference between the C:N ratio of aggregates and suspended cells (Tukey HSD, $p = 0.2847$).

TEP carbon (TEP-C_{color}) as estimated from TEP_{color} contributed <5% to total POC during the stationary phase in all treatments (Fig. 9). During senescence, TEP-C contributed 14, 8 and 8% of POC in the f/2, f/2-N and f/2-Si treatment, respectively.

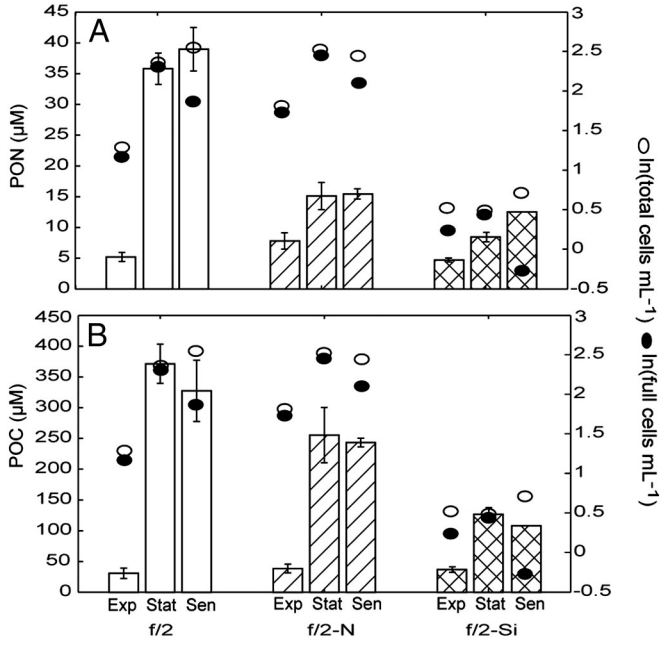

Fig. 8. Elemental composition of *Coscinodiscus wailesii* under different nutrient concentrations. A) POC and B) PON and total and live cell concentrations in different experimental treatments (f/2, f/2-N and f/2-Si) during exponential (Exp) stationary (Stat) and senescent phase (Sen). Error bars represent one standard deviation from the mean ($n = 3$) except in the scenescent f/2-Si treatment (one sample from 3 pooled replicate treatments).

4. Discussion

4.1. Growth of C. wailesii under different nutrient conditions and implications for the diatom's life-history

Growth, senescence and aggregation of *C. wailesii* cultures was followed in incubations with three different initial silicic acid and nitrate concentrations and nutrient Si:N ratios through addition of silicic acid and nitrate (f/2 media), Si alone (f/2-N treatment) or nitrate alone (f/2-Si treatment) to natural North Sea water. In all treatments *C. wailesii* was Si limited towards the end of the experiment and possibly Si and N co-limited in the f/2-N treatment. The potential Si and N co-limitation was consistent with the high C:N ratios during stationary and senescent phases in f/2-N as compared to f/2 and f/2-Si and seemed to have retarded death in *C. wailesii* (as suggested by the linear increase in dead cells towards the end of the experiment vs. an exponential increase in f/2 and f/2-Si).

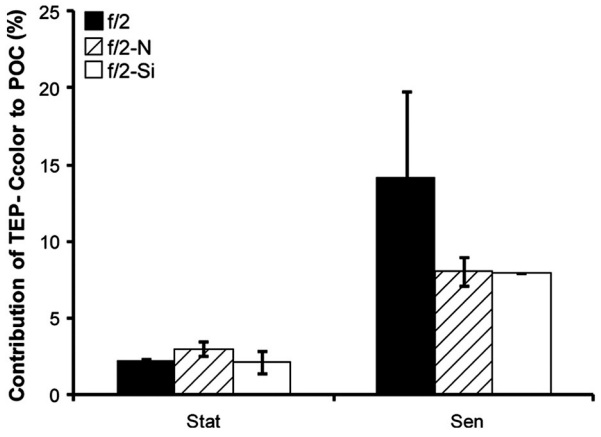

Fig. 9. Carbon contribution of TEP (TEP-C_{color}) produced by *Coscinodiscus wailesii*. Mean fraction of TEP-C_{color} to the total POC (given in % of total POC) determined for *C. wailesii* grown under nutrient-replete (f/2), nitrogen-reduced (f/2-N), and silicic acid-limited (f/2-Si) conditions during stationary (Stat) and senescent (Sen) phases. Each error bar represents 1 standard deviation from the mean. Each $n = 3$ except $n_{f/2} = 2$.

Division rates in the f/2-Si treatment were significantly lower than those in the f/2 and f/2-N treatments. However, cell concentrations showed a steady increase well after f/2 and f/2-N cultures had reached the stationary phase, implying that *C. wailesii* can sustain growth at low Si concentrations. From the molar uptake ratios under non Si-limiting conditions (Table 1) we estimate the Si:N ratio of *C. wailesii* to be at least double the average diatom ratio of 1:1 (Brzezinski, 1985; Quéguiner et al., 1997), which is in line with estimates of 2.4:1 to 5.2:1 determined for natural *C. wailesii* cells of the Seto Inland Sea, Japan (Ono et al., 2008). Post-bloom Si concentrations in the Seto Inland Sea were reduced to <3 μM Si illustrating the exceptionally high Si demand of *C. wailesii*. The implication for the North Sea is that blooms of *C. wailesii* are capable of utilizing at least twice the amount of Si than indigenous diatoms.

The high silicic acid demand of *C. wailesii* has two consequences: First, the large size and thick-walled frustules of *C. wailesii* evidently provide mechanical protection against ingesting predators (Friedrichs et al., 2013). It is too large to be ingested by the common coastal copepod *Acartia* (Friedrichs et al., 2013). Another common coastal copepod species, *Temora longicornis*, is able to bite off a piece from the frustule and suck out the cell contents (Jansen, 2008). Under iron-limitation, elevated cellular silica content of *C. wailesii* is associated with a reduction in valve pore size, thereby increasing the mechanical resistance of the frustule and its effectiveness as a defense mechanism against predators (Wilken et al., 2011). Second, the Si requirement of *C. wailesii* restricts its abundance to seasons when silicic acid is high, i.e. during winter–spring transition and following autumnal mixing. This matches observations of *C. wailesii* blooms in the past: *C. wailesii* was first reported in European waters in January (Boalch and Harbour, 1977) with a subsequent bloom resulting in massive mucilage formation during April. A late winter bloom of *C. wailesii* was reported in the Bay of Biscay during March 2001 also causing heavy mucilage production when the bloom declined (Gohin et al., 2003). A review of *C. wailesii* occurrence in the German Bight found that >90% of phytoplankton carbon was contributed by *C. wailesii* between December 1988 and March 1989 (Rick and Duerselen, 1995). The authors also found the species in autumn. As diatom frustules are only a minor fraction of North Sea surface sediments one can assume that the bulk dissolve with time and the Si is returned to the water column during autumnal mixing. Uptake of Si by *C. wailesii* during winter–spring transition will restrict biomass build-up of diatoms during the spring bloom, which might alter the established local species succession (Ono et al., 2008). For example, the excess N and P will result in a shift of dominance to non-diatom phytoplankton such as phytoflagellates or the colony-forming prymnesiophyte *Phaeocystis* with important ramifications for pelagic food web structure.

4.2. Aggregate formation in C. wailesii under different nutrient conditions

We found that compact and rounded or diffuse and elongated filamentous aggregates, of up to 10 cm in length, formed in every treatment except under silicic acid limitation (in each of the triplicates of batches 1 and 2). Thus, under our experimental conditions, the high biomass, reached under f/2 and f/2-N conditions seemed to be a prerequisite for aggregate formation. The examination of aggregates by microscopy revealed that they consisted of live and dead cells and empty frustules embedded in exuded, autolysed cytoplasm that constituted the binding agent of the aggregates formed. These results imply that cell death and lysis play a substantial role in triggering aggregate formation. These results are supported by POC and PON measurements, indicating that elemental composition of particulate matter was similar in aggregates and solitary cells. Extensive autolysis involving cell wall- and cytoskeleton-free cytoplasm of different auto- and heterotrophic protists has been previously correlated to massive mucilage events (Baldi et al., 1997; Brussaard et al., 1997). Additionally, the brownish colour of the released material, due to incorporation of chloroplast pigments, fits descriptions of the mucilage produced by natural *C. wailesii* populations (Boalch and Harbour, 1977).

Besides the large aggregates that formed during the stationary and senescent phases, we observed small aggregates (20–50 cells) occurring sporadically in the f/2 and f/2-N treatments during the exponential phase suggesting that individual diatom frustules must also have adhesive properties. Although we did not measure the stickiness of *C. wailesii* cells in our experiments, adhesiveness of *C. wailesii* cells is further supported by the observation of a polysaccharidic layer covering the frustule that might be of sticky nature and involved in coagulation processes of *C. wailesii*.

4.3. TEP production of C. wailesii during aggregate formation

Cellular TEP production in the f/2-Si treatments was significantly higher than TEP produced by *C. wailesii* in the other two treatments. Since the cells were much more densely packed with chloroplasts than other treatments (Fig. 3), it appears that cell division was inhibited by lack of sufficient Si (Brzezinski et al., 1990). Consequently, prolonged silicic acid limitation inhibiting cell division of *C. wailesii*, leads to the release of excess photosynthates in the form of TEP. In the other treatments (in particular in f/2) TEP concentrations also increased significantly towards the end of the experiment when cultures also reached Si limitation. Conversely, noticeable brownish mucilaginous material released from dead cells, although observed in all treatments, accumulated exclusively in treatments with high initial silicic-acid concentrations that allowed the buildup of high biomass. The POC/PON ratio of aggregates did not differ significantly from that of suspended cells suggesting that the former did not contain much additional carbohydrates in the form of TEP. Hence, TEP release in *C. wailesii* is not generated as a consequence of mass cell lysis during bloom collapse. Further, the fact that aggregate formation did not take place in the Si-limited treatment (f/2-Si) during senescence at similar TEP concentrations as stationary phase of other treatments (f/2 and f/2-N) where aggregation occurred, indicates that aggregate formation might not necessarily be related to TEP abundance but rather to the release of intracellular material after cell lysis at high cell densities.

4.4. The polysaccharidic layer

The existence of an organic layer encasing diatom frustules is well known and has been widely studied (e.g. Hecky et al., 1973; Reimann et al., 1965, 1966). According to these and further investigations the layer consists of polysaccharides (Waite et al., 1995) as well as proteins (Hecky et al., 1973), of which the latter serve to protect the diatom as they constitute a template for silicification of the frustule and prevent rapid silica dissolution (Bidle and Azam, 1999). Considering that the moulds, sloughed off by dead *C. wailesii* cells, resembled “blueprints” of the frustule-indicates that the organic layer of *C. wailesii* serves as a silicification template. The intense staining by AB might furthermore be indicative of an exceptionally dense packing of polysaccharides, potentially protecting the cells from bacterial degradation. A possible function of the cell coating as a defense mechanism, as well as the size of the diatom, which prevents larger predators from consuming it, might contribute to the success of *C. wailesii* as an invasive species.

5. Conclusions

In *C. wailesii*, release of autolysed cytoplasm and subsequent aggregate formation was observed under final Si-limitation (f/2) and Si–N co-limitation (f/2-N), i.e. in treatments which had built up high cell densities during the exponential growth phase. In contrast, no such aggregates were formed in continuously Si limited (f/2-Si) treatments, which were characterised by low cell densities. Although TEP occurred in all treatments, in particular during stationary and senescent phases, TEP production in *C. wailesii* was increased under Si limitation. This

suggests that aggregation in *C. wailesii* seemed more dependent on cell concentration and mortality, and that autolysed cytoplasm released after cell death is the major binding agent of *C. wailesii* aggregates.

Acknowledgements

This work was conducted at the Alfred Wegener Institute Helmholtz Center for Polar and Marine Research (AWI) in Bremerhaven and the Biologische Anstalt Helgoland (BAH), Germany. We are grateful for the support from the staff at both locations and in particular we thank N. Aberle-Malzahn, A. Kraberg and M. Loeder for their support during sampling and establishment of *Coscinodiscus wailesii* cultures. Furthermore we highly appreciate the advice and assistance from A. Engel, M. Wurst and T. Mattfeldt for the TEP analyses. We thank C. Lorenzen and S. Rokitta for support with the POC and PON analysis. **[SS]**

References

Alcoverro, T., Conte, E., Mazzella, L., 2000. Production of mucilage by the Adriatic epipelic diatom *Cylindrotheca closterium* (Bacillariophyceae) under nutrient limitation. J. Phycol. 36 (6), 1087–1095.

Alldredge, A.L., Passow, U., Logan, B.E., 1993. The abundance and significance of a class of large, transparent organic particles in the Ocean. Deep Sea Res. I Oceanogr. Res. Pap. 40 (6), 1131–1140.

Assmy, P., Smetacek, V., Montresor, M., Klaas, C., Henjes, J., Strass, V.H., Arrieta, J.M., Bathmann, U., Berg, G.M., Breitbarth, E., Cisewski, B., Friedrichs, L., Fuchs, N., Herndl, G.J., Jansen, S., Krägefsky, S., Latasa, M., Peeken, I., Röttgers, R., Scharek, R., Schüller, S.E., Steigenberger, S., Webb, A., Wolf-Gladrow, D., 2013. Thick-shelled, grazer-protected diatoms decouple ocean carbon and silicon cycles in the iron-limited Antarctic Circumpolar Current. Proc. Natl. Acad. Sci. U. S. A. http://dx.doi.org/10.1073/pnas.1309345110 (Early Edition).

Azetsu-Scott, K., Passow, U., 2004. Ascending marine particles: significance of transparent exopolymer particles (TEP) in the upper ocean. Limnol. Oceanogr. 49 (3), 741–748.

Baldi, F., Minacci, A., Saliot, A., Mejanelle, L., Mozetic, P., Turk, V., Malej, A., 1997. Cell lysis and release of particulate polysaccharides in extensive marine mucilage assessed by lipid biomarkers and molecular probes. Mar. Ecol. Prog. Ser. 153, 45–57.

Bidle, K.D., Azam, F., 1999. Accelerated dissolution of diatom silica by marine bacterial assemblages. Nature 397 (6719), 508–512.

Bidle, K.D., Bender, S.J., 2008. Iron starvation and culture age activate metacaspases and programmed cell death in the marine diatom *Thalassiosira pseudonana*. Eukaryot. Cell 7, 223–236.

Bidle, K.D., Falkowski, P.G., 2004. Cell death in planktonic, photosynthetic microorganisms. Nat. Rev. Microbiol. 2 (8), 643–655.

Boalch, G.T., Harbour, D.S., 1977. Unusual diatom off coast of south-west England and its effects on fishing. Nature 269, 687–688.

Bratbak, G., Egge, J.K., Heldal, M., 1993. Viral mortality of the marine alga *Emiliania huxleyi* (Haptophyceae) and termination of algal blooms. Mar. Ecol. Prog. Ser. 93, 39–48.

Brussaard, C.P.D., Noordeloos, A.A.M., Riegman, R., 1997. Autolysis kinetics of the marine diatom *Ditylum brightwellii* (Bacillariophyceae) under nitrogen and phosphorus limitation and starvation. J. Phycol. 33 (6), 980–987.

Brzezinski, M.A., 1985. The Si:C:N ratio of marine diatoms: interspecific variability and the effect of some environmetal variables. J. Phycol. 21 (3), 347–357.

Brzezinski, M.A., Conley, D.J., Olson, R.J., Chisholm, S.W., 1990. Silicon availability and cell-cycle progression in marine diatoms. Mar. Ecol. Prog. Ser. 67, 83–96.

Decho, A.W., 1990. Microbial exopolymer secretions in ocean environments: their role(s) in food webs and marine processes. In: Barnes, H.a.M. (Ed.), Oceanography and Marine Biology—An Annual Review. Aberdeen University Press.

Edwards, M., John, A.W.G., Johns, D.G., Reid, P.C., 2001. Case history and persistence of the non-indigenous diatom *Coscinodiscus wailesii* in the North-East Atlantic. J. Mar. Biol. Assoc. U. K. 81 (2), 207–211.

Engel, A., 2009. Determination of Marine Gel Particles. Practical Guidelines for the Analysis of Seawater. Taylor & Francis Group, Boca Raton, Florida, pp. 125–142.

Engel, A., Passow, U., 2001. Carbon and nitrogen content of transparent exopolymer particles (TEP) in relation to their Alcian Blue adsorption. Mar. Ecol. Prog. Ser. 219, 1–10.

Friedrichs, L., Hörnig, M., Schulze, L., Bertram, A., Jansen, S., Hamm, C., 2013. Size and biomechanic properties of diatom frustules influence food uptake by copepods. Mar. Ecol. Prog. Ser. 481, 41–51.

Fuhrmann, J.A., 1999. Marine viruses and their biogeochemical and ecological effects. Nature 399, 541–548.

Fukao, T., Kimoto, K., Yamatogi, T., Yamamoto, K.I., Yoshida, Y., Kotani, Y., 2009. Marine mucilage in Ariake Sound, Japan, is composed of transparent exopolymer particles produced by the diatom *Coscinodiscus granii*. Fish. Sci. 75 (4), 1007–1014.

Geider, R.J., Roche, J.L., 2002. Redfield revisited: variability of C:N:P in marine microalgae and its biochemical basis. Eur. J. Phycol. 37 (01), 1–17.

Gohin, F., Lampert, L., Guillaud, J.F.O., Herbland, A., Nezan, E., 2003. Satellite and in situ observations of a late winter phytoplankton bloom, in the northern Bay of Biscay. Cont. Shelf Res. 23 (11–13), 1117–1141.

Grasshoff, K., Kremling, K., Ehrhardt, M., 1999. Methods of Seawater Analysis, third ed. Wiley-VCH Verlag GmbH, Weinheim, Germany.

Guillard, R.R.L., Ryther, J.H., 1962. Studies on marine planktonic diatoms. *Cyclotella nana* Hustedt, and *Detonula confervacea* (Cleve) Gran. Can. J. Microbiol. 8, 229–239.

Hamm, C.E., 2002. Interactive aggregation and sedimentation of diatoms and clay-sized lithogenic material. Limnol. Oceanogr. 47 (6), 1790–1795.

Hargraves, P.E., French, F.W., 1983. Diatom resting spores: significance and strategies. In: Fryxell, G.A. (Ed.), Survival Strategies of the Algae. Cambridge University Press, Cambridge, pp. 49–68.

Hecky, R.E., Kilham, P., 1988. Nutrient limitation of phytoplankton in freshwater and marine environments: a review of recent evidence on the effects of enrichment. Limnol. Oceanogr. 33 (4), 796–822.

Hecky, R.E., Mopper, K., Kilham, P., Degens, E.T., 1973. The amino acid and sugar composition of diatom cell-walls. Mar. Biol. 19 (4), 323–331.

Hewes, C.D., Holm-Hansen, O., 1983. A method for recovering nanoplankton from filters for identification with the microscope: the filter-transfer-freeze (FTF) technique. Limnol. Oceanogr. 28 (2), 389–394.

Jansen, S., 2008. Copepods grazing on *Coscinodiscus wailesii*: a question of size? Helgol. Mar. Res. 62 (3), 251–255.

Lancelot, C., 1995. The mucilage phenomenon in the continental coastal waters of the North-Sea. Sci. Total Environ. 165 (1–3), 83–102.

Myklestad, S., 1974. Production of carbohydrates by marine planktonic diatoms. I. Comparison of nine different species in culture. J. Exp. Mar. Biol. Ecol. 15 (3), 261–274.

Myklestad, S.M., 1995. Release of extracellular products by phytoplankton with special emphasis on polysaccharides. Sci. Total Environ. 165 (1–3), 155–164.

Ono, A., Tada, K., Ichimi, K., 2008. Chemical composition of *Coscinodiscus wailesii* and the implication for nutrient ratios in a coastal water, Seto Inland Sea, Japan. Mar. Pollut. Bull. 57 (1–5), 94–102.

Passow, U., 2002. Transparent exopolymer particles (TEP) in aquatic environments. Prog. Oceanogr. 55 (3–4), 287–333.

Passow, U., Alldredge, A.L., 1994. Distribution, size and bacterial colonization of transparent exopolymer particles (TEP) in the ocean. Mar. Ecol. Prog. Ser. 113 (1–2), 185–198.

Passow, U., Alldredge, A.L., 1995. A dye-binding assay for the spectrophotometric measurement of transparent exopolymer particles (TEP). Limnol. Oceanogr. 40 (7), 1326–1335.

Passow, U., Shipe, R.F., Murray, A., Pak, D.K., Brzezinski, M.A., Alldredge, A.L., 2001. The origin of transparent exopolymer particles (TEP) and their role in the sedimentation of particulate matter. Cont. Shelf Res. 21 (4), 327–346.

Percival, E., Anisur Rahman, M., Weigel, H., 1980. Chemistry of the polysaccharides of the diatom *Coscinodiscus nobilis*. Phytochemistry 19 (5), 809–811.

Quéguiner, B., Tréguer, P., Peeken, I., Scharek, R., 1997. Biogeochemical dynamics and the silicon cycle in the Atlantic sector of the Southern Ocean during austral spring 1992. Deep Sea Res. II Top. Stud. Oceanogr. 44 (1–2), 69–89.

Reimann, B.E.F., Lewin, J.C., Volcani, B.E., 1965. Studies on the biochemistry and fine structure of silica shell formartion in diatoms. J. Cell Biol. 24 (1), 39–55.

Reimann, B.E.F., Leivin, J.C., Volcani, B.E., 1966. Studies on the biochemistry and fine structure of silica shell formartion in diatoms. II. The structure of the cell wall of *Navicula pelliculosa* (Bréb.) Hilse. J. Phycol. 2 (2), 74–84.

Rick, H.J., Duerselen, C.D., 1995. Importance and abundance of the recently established species *Coscinodiscus wailesii* Gran & Angst in the German Bight. Helgoländer Meeresun. 49, 355–374.

Smetacek, V.S., 1985. Role of sinking in diatom life-history cycles: ecological, evolutionary and geological significance. Mar. Biol. 84 (3), 239–251.

Thornton, D.C.O., 2002. Diatom aggregation in the sea: mechanisms and ecological implications. Eur. J. Phycol. 37, 149–161.

Uren, A.G., O'Rourke, K., Aravind, L., Pisabarro, M.T., Seshagiri, S., Koonin, E.V., Dixit, V.M., 2000. Identification of paracaspases and metacaspases: two ancient families of caspase-like proteins, one of which plays a key role in MALT lymphoma. Mol. Cell 6 (4), 961–967.

Vardi, A., Berman-Frank, I., Rozenberg, T., Hadas, O., Kaplan, A., Levine, A., 1999. Programmed cell death of the dinoflagellate *Peridinium gatunense* is mediated by CO_2 limitation and oxidative stress. Curr. Biol. 9 (18), 1061–1064.

Veldhuis, M.J.W., Kraay, G.W., Timmermans, K.R., 2001. Cell death in phytoplankton: correlation between changes in membrane permeability, photosynthetic activity, pigmentation and growth. Eur. J. Phycol. 36 (2), 167–177.

Waite, A.M., Olson, R.J., Dan, H.G., Passow, U., 1995. Sugar-containing compounds on the cell surfaces of marine diatoms measured using concanavalin A and flow cytometry. J. Phycol. 31 (6), 925–933.

Wilken, S., Hoffmann, B., Hersch, N., Kirchgessner, N., Dieluweit, S., Rubner, W., Hoffmann, L.J., Merkel, R., Peeken, I., 2011. Diatom frustules show increased mechanical strength and altered valve morphology under iron limitation. Limnol. Oceanogr. 56 (4), 1399–1410.